Biogeochemistry
DOI 10.1007/s10533-013-9911-8

Biogenic silica recycling in sea ice inferred from Si-isotopes: constraints from Arctic winter first-year sea ice

François Fripiat · Jean-Louis Tison · Luc André · Dirk Notz · Bruno Delille

Received: 9 May 2013 / Accepted: 11 September 2013

Abstract We report silicon isotopic composition (δ^{30}Si vs. NBS28) in Arctic sea ice, based on sampling of silicic acid from both brine and seawater in a small Greenlandic bay in March 2010. Our measurements show that just before the productive period, δ^{30}Si of sea-ice brine similar to δ^{30}Si of the underlying seawater. Hence, there is no Si isotopic fractionation during sea-ice growth by physical processes such as brine convection. This finding brings credit and support to the conclusions of previous work on the impact of biogenic processes on sea ice δ^{30}Si: any δ^{30}Si change results from a combination of biogenic silica production and dissolution. We use this insight to interpret data from an earlier study of sea-ice δ^{30}Si in Antarctic pack ice that show a large accumulation of biogenic silica. Based on these data, we estimate a significant contribution of biogenic silica dissolution (D) to production (P), with a D:P ratio between 0.4 and 0.9. This finding has significant implications for the understanding and parameterization of the sea ice Si-biogeochemical cycle, i.e. previous studies assumed little or no biogenic silica dissolution in sea ice.

Keywords Sea ice · Nutrient cycles · Silicon · Biogenic silica production · Biogenic silica dissolution

Responsible Editor: Leila J. Hamdan.

F. Fripiat (✉) · J.-L. Tison
Department of Earth and Environmental Sciences, Université Libre de Bruxelles, 1050 Brussels, Belgium
e-mail: ffripiat@ulb.ac.be

F. Fripiat · J.-L. Tison
Earth System Sciences & Analytical and Environmental Chemistry, Vrije Universiteit Brussel, Brussels, Belgium

L. André
Department of Earth Sciences, Royal Museum for Central Africa, Tervuren, Belgium

D. Notz
Max Planck Institute for Meteorology, Hamburg, Germany

B. Delille
Unité d'Océanographie Chimique, Interfacultary Center for Marine Research, Université de Liège, Liège, Belgium

Introduction

Polar ecosystems play an important role for the regulation of biogeochemical cycles and climate at global scale. Sea ice accounts for up to 25 % of total primary production in sea-ice covered waters (including the highly productive marginal ice zone, Legendre et al. 1992; Arrigo and Thomas 2004) and exceeds 50 % in perennially ice-covered water (Gosselin et al. 1997). Sea-ice primary production is usually dominated by diatoms (Thomas and Dieckmann 2002). These are unicellular algae that require silicic acid ($Si(OH)_4$) to build their cell walls, which are made of biogenic silica (referred to as frustules, $bSiO_2$). While

Published online: 06 October 2013

it is generally acknowledged that sea ice significantly impacts the biogeochemical dynamics in polar oceans, little information still exists on the relative contribution of the different processes (i.e. assimilation, regeneration, export) and on their seasonal evolution (Thomas et al. 2010). Such lack of data mainly originates from the challenges in manipulating the micro-organisms thriving within sea ice, e.g. to perform incubations without altering the environment.

The isotopic composition of silicon is a valuable proxy to help addressing this issue. During silicic acid consumption by diatoms, the lighter Si isotope (^{28}Si) is consumed preferentially, leaving the residual silicic acid pool enriched in the heavy Si-isotope (^{30}Si; De La Rocha et al. 1997). Such preferential incorporation of ^{28}Si into biogenic silica is described by a fractionation factor $^{30}\varepsilon$ that is equivalent to the ratio of the reaction rate of the heavy (^{30}k) and light (^{28}k) Si-isotopes (=[^{30}k:^{28}k]−1, reported in permil units, ‰). Field-based estimate of the fractionation factor is -1.2 ± 0.3 ‰ (De La Rocha et al. 2000, 2011; Varela et al. 2004; Cardinal et al. 2005; Reynolds et al. 2006; Beucher et al. 2008; Cavagna et al. 2011; Fripiat et al. 2011). Sutton et al. (2013) recently provided evidence that Si isotope fractionation by diatoms is species-dependent, with estimates of in vitro $^{30}\varepsilon$ varying from −0.5 to −2.1 ‰. The narrower range for estimates of in situ $^{30}\varepsilon$ indicates that naturally mixed diatom assemblages have the ability to partly erase the species specific variability, as was also found for nitrate assimilation (Sigman et al. 2009). Biogenic silica dissolution preferentially releases light ^{28}Si isotopes ($^{30}\varepsilon = -0.55 \pm 0.05$ ‰; Demarest et al. 2009), thereby dampening the overall net isotopic fractionation associated with net biogenic silica production. For a given set of conditions, the mass and isotopic balance can be analyzed to derive insights into the dominant biogeochemical processes and to quantify the related fluxes (de Brauwere et al. 2012).

A major obstacle for any attempt to use sea ice δ^{30}Si data to unravel sea-ice associated Si-biogeochemical dynamic lies in the lack of sufficient data that describe the initial distribution of δ^{30}Si in newly formed sea ice. In this study we address this issue by presenting and analyzing silicic acid δ^{30}Si measurements as obtained in newly formed Arctic sea ice. Our data, sampled in March 2010, allow for a better understanding of the processes that drive the distribution of δ^{30}Si before the onset of the productive period that usually lasts from April to June. As an application of these new insights into initial silicon dynamic, we analyze data from a previous Antarctic field campaign to quantify the contribution of $bSiO_2$ dissolution to production.

This paper is organized as follows. In the following section, we describe the field setting and our methods. In "Results of Arctic field measurements" section, we present and discuss the data from the Arctic field work, while "The contribution of dissolution to production" section contains our analysis of the Antarctic data. The paper closes with a summary of our main results.

Materials and methods

To enhance our understanding of the formation, growth and decay of first-year sea ice, a winter-long international research campaign was carried out in the proximity of the settlement of Upernavik (∼72°79′N, 56°06′W) in Western Greenland in winter 2009/2010. The German sailing vessel 'SS Dagmar Aaen' was anchored in a bay there throughout winter (bay area ∼120 vs. 100 m^2, average depth = 8 m), and was from February 2010 onwards surrounded by newly forming first-year sea ice (Fig. 1). Oceanic currents were almost absent in the bay and surrounding mountains protected the bay from wind (Ehlert 2012).

The main sampling period described in this study lasted from 13 to 26 March 2010. On the first and the last day of this period, a sea-ice core was extracted from the ice to determine profiles of ice temperature and ice bulk salinity. Ice temperature was measured in situ directly after extraction of the cores, using a calibrated probe (Greisinger GTH 175) inserted in pre-drilled holes (perpendicular to core sides) at the exact diameter of the probe and with a depth resolution of 5 cm. For ice salinity, melted ice samples were collected from successive 5 cm thick slices of the core and were measured with a portable conductivity meter (Hach HQ40d) with a precision of ±0.1 g kg^{-1}.

Brine and seawater for δ^{30}Si and chlorophyll-*a* analysis were sampled at 1–2 day intervals throughout our sampling period ($n = 9$). For these measurements, an undisturbed sampling area of 15 m × 30 m was selected in the existing first-year ice (Fig. 1b). Within this area, small 1 m × 2 m sub-areas were chosen for the individual samplings.

Brine samples were collected using the sackhole sampling technique in which brine is allowed to

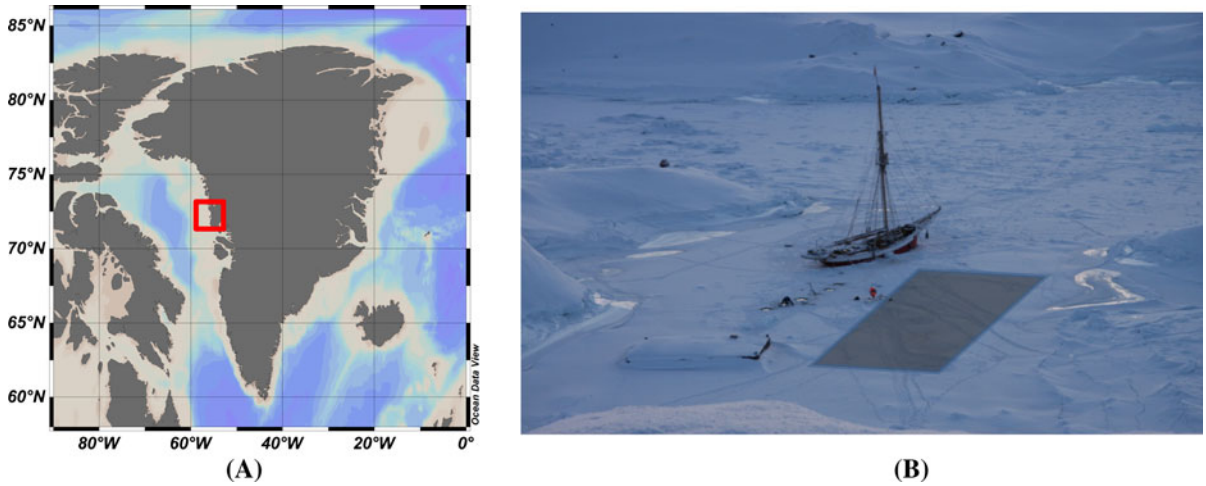

Fig. 1 **a** Location of the sample site (*red square*) and **b** general view of the sampling area (~*gray rectangle*). (Color figure online)

percolate into partial core holes ($n = 4$). A sufficient brine volume of about 1 l was collected over a 20–40 min long interval in covered core holes that had a diameter of 10 cm and a bottom at about 10 cm above the ice–ocean interface. Average brine salinity was 91 ± 7 g kg^{-1}, indicating no significant invasion by seawater and relatively pure brine sampling. About 1 l of seawater was sampled by inserting sampling bottles into the underlying seawater through a 40 cm by 40 cm large hole that was cut into the ice.

Samples of both brine and seawater were immediately filtered on Nuclepore polycarbonate membranes (0.4 µm porosity) using a polycarbonate syringe and polycarbonate filter (Ø = 47 mm) header. Filtered water samples for silicic acid analysis were stored in acid-cleaned polyethylene (PE) bottles at room temperature. A fraction of the collected water (350 ml) was dedicated to chlorophyll-*a* (chl-*a*) measurement and filtered on precombusted Whatman GF/F filters using polycarbonate syringe and polycarbonate filter (Ø = 47 mm) header.

Samples were processed back in the home laboratory (ULB, Brussels; RMCA, Tervuren; ULg, Liège). The measurements of chl-*a* were carried out following the recommendations of Arar and Collins (1997) with a Turner Design TD700 fluorometer. $Si(OH)_4$ concentration were measured with an Inductively Coupled Plasma Atomic Emission Spectrometer (ICP-AES, Thermo Optek Iris Advantage, RMCA) with a relative standard deviation <5 %.

For δ^{30}Si analysis, silicic acid was co-precipitated with triethylamine molybdate (De La Rocha et al. 1996) with a minimum Si requirement of 1.5 µmol. After combustion of the precipitated silicomolybdate in covered Pt crucibles at 1,000 °C, the resulting pure cristobalite SiO_2 was transferred to pre-cleaned PP vials. SiO_2 was dissolved in a dilute HF/HCl mixture as described in Cardinal et al. (2003). Silicon isotopic composition was determined with a MultiCollector Inductively Coupled Plasma Mass Spectrometer (MC-ICP-MS, Nu Plasma; ULB-RMCA), using Mg external doping in dry plasma mode following Abraham et al. (2008). We report the silicon isotopic composition relative to a standard (NBS28) which is analyzed immediately after and before the sample, using the delta value (‰) as defined by:

$$\delta^{30}Si = \left(\frac{\left({}^{30}Si/{}^{28}Si\right)_{sample}}{\left({}^{30}Si/{}^{28}Si\right)_{NBS28}} - 1 \right) \times 1{,}000 \qquad (1)$$

The average precision and reproducibility of the measurements are ±0.1 ‰ (±1SD) for δ^{30}Si (Reynolds et al. 2007). The accuracy of the measurements was checked daily on secondary reference materials (e.g. Diatomite) with known Si isotopic compositions resulting from an inter-comparison exercise (Reynolds et al. 2007). Each analysis was duplicated from the post-sampling processing to the isotopic measurement.

Similar to the concentration of initial seawater salinity in sea-ice brine, nutrient distribution in the brine changes by temperature-induced dilution or concentration during melting and freezing processes within sea ice. To correct for these effects, all measured concentrations in the brine were

normalized to the salinity of underlying seawater according to:

$$\mathrm{conc_{norm}} = \mathrm{conc_{brine}} \times \frac{S_{seawater}}{S_{brine}} \quad (2)$$

Here, $\mathrm{conc_{norm}}$ is the normalized concentration, $\mathrm{conc_{brine}}$ the measured concentration in the brine, $S_{seawater}$ is the salinity of seawater and S_{brine} is the measured brine salinity.

Results of Arctic field measurements

The sea ice at our sampling site was less than 2 month old at the time of sampling in mid-March. It had an average thickness of 32 ± 5 cm ($n = 16$) and was covered by 5 ± 2 cm of snow ($n = 10$). Its brine salinity, as derived from temperature profiles based on the assumption of thermodynamic equilibrium (Cox and Weeks 1983), was decreasing downward from up to 159.7 to 31.8 g kg^{-1}, close to the seawater values of 33.8 g kg^{-1}. Brine volumes as calculated from these brine salinities and the measured bulk salinities ranged between 4.8 and 13.9 %, and are hence in a range that is often associated with a permeable interconnected brine network (e.g., Petrich et al. 2006).

Brine chl-*a* concentration varied from 0.01 to 0.33 µg l^{-1}, well below the range of 3–800 µg l^{-1} that is generally encountered in Arctic sea ice (Arrigo et al. 2010). The low values at our field site are indicative for the lack of significant primary production prior to or during our sampling period in mid-March. This is consistent with other studies, which found that extensive accumulation of sea ice biomass in Arctic first-year sea ice is usually observed from April to June following the onset of the ice-algal bloom (Horner and Schrader 1982; Lee et al. 2008; Riedel et al. 2008). Low chl-*a* concentration at our field site was also observed in the underlying seawater (0.00–0.18 µg l^{-1}), suggesting also low seawater primary production.

Normalized brine silicic acid concentration (25.1 ± 1.6 µmol l^{-1}) was, within error bars, identical to seawater silicic acid concentration (25.7 ± 1.3 µmol l^{-1}; Fig. 2). Silicic acid δ^{30}Si was also undistinguishable from underlying seawater (Fig. 2), its values being 1.9 ± 0.1 and 1.9 ± 0.2 ‰, respectively. These measurements can be understood as follows. As seawater freezes, only its freshwater content freezes to form solid ice crystals. The salt that is dissolved in the seawater is not embedded into the crystal matrix, but gets instead more and more concentrated in the remaining interstitial, liquid brine. This process continuous until the salt concentration is large enough to reach phase equilibrium as given by the local temperature. In a similar way, nutrients that are contained in seawater become more and more concentrated in the brine. In particular, if the normalized concentration of any nutrient as given by Eq. (2) is equal to the concentration found in the source seawater, we can infer that this particular nutrient was simply passively concentrated in the brine. In our case, the fact that normalized brine silicic acid concentration is equal in brine and in seawater hence means that there was neither significant biogenic silica production and/or dissolution within the brine network, nor significant lithogenic silica dissolution. The constant value of silicic acid δ^{30}Si additionally implies that there was no discrimination of silicon isotopes by physical processes.

Our measurements strongly indicate that these findings not only hold for brine that has only just been formed close to the ice–ocean interface, but also for brine that was isolated from the underlying seawater since the initial formation of sea ice, in our case for almost 2 months. While we did not measure brine convection in our field setup directly, theoretical considerations and model simulations strongly indicate that brine convection in first-year growing sea ice only occurs very close to the ice–ocean interface, where most of the brine loss from sea ice occurs (Griewank and Notz 2013). This is related to the fact that convectional brine loss from sea ice, so-called gravity drainage, only occurs once a sufficiently unstable vertical density gradient of the brine goes

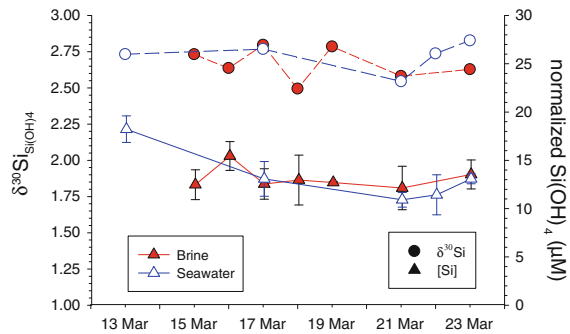

Fig. 2 Normalized $Si(OH)_4$ concentration (*dot connected by dashed lines*) and isotopic composition (*triangle connected with full lines*) for both brine (*red*) and underlying seawater (*blue*). (Color figure online)

along with a sufficiently high permeability of the ice (Worster and Wettlaufer 1997; Notz and Worster 2009). Whenever both these conditions are met, brine is replaced by convection against underlying seawater. Some of the intruding seawater will freeze within the sea ice, since the seawater is less salty than the brine it replaces. This then lowers permeability, and convection ceases. Close to the ice–ocean interface, permeability is so large that convection is almost continuously maintained. Further into the ice, however, the permeability is so low that the existing brine-density gradient is no longer sufficient to trigger convection: the brine remains isolated from the underlying seawater. As a result, brine moves very little in the interior of the ice throughout winter, and the interior of the ice in winter can usually be approximated as a closed system. Episodic full-depth convection within sea ice will only set in once the ice has warmed sufficiently in spring to increase permeability throughout the entire ice thickness (Jardon et al. 2013; Griewank and Notz 2013). Based on this reasoning, we deduce that our measurements are representative both for brine that has only recently been formed in sea ice (namely close to the ice–ocean interface) and for brine that was isolated from the underlying seawater for some time (namely higher up in the ice): for both cases, normalized concentrations of silica acid and silicic acid δ^{30}Si are virtually identical to those measured in the source seawater. Hence, before the onset of significant production, both can be interpreted simply as passive tracers that are concentrated in the same way as salinity in the brine as sea ice forms. Any silicon isotopic alteration relative to the source seawater must therefore be caused by biogenic silica production and dissolution, which can hence be quantified as outlined in the following section.

The contribution of dissolution to production

Fripiat et al. (2007) reported a biogenic silica δ^{30}Si between 0.8 and 1.7 ‰ for productive Antarctic first-year pack ice, in the Australian Southern Ocean sector. Using the recent estimate for the $bSiO_2$ dissolution fractionation factor (−0.55 ‰; Demarest et al. 2009), our analysis of the Arctic field data puts us in the position of constraining the contribution of $bSiO_2$ dissolution to production in the final observed δ^{30}Si signature of the Fripiat et al. (2007) dataset. From that dataset, we use three available bulk ice samples with both known silicic acid concentration and biogenic silica δ^{30}Si: one bottom community found in columnar ice at the ice–ocean interface (station IV; sea ice and snow thickness of 48 and 2 cm, respectively); one surface snow ice community at the interface with the atmosphere (station V; sea ice and snow thickness of 80 and 20 cm, respectively); and another surface snow ice community (station III, sea ice and snow thickness of 155 and 25 cm, respectively). Columnar ice refers to vertically elongated crystals formed by downward sea ice growth under quiescent conditions. Snow ice forms by the refreezing of slush at the snow–ice interface. This slush originates from the infiltration (=flooding) of seawater at the base of the snow pack when snow is thick enough to depress the ice surface below sea level (e.g. Maksym and Markus 2008).

We use a time-dependent geochemical single-box model of sea-ice brine to constrain the relative rate of biogenic silica dissolution. The model simulates the change in both silicic acid concentration and δ^{30}Si within the brine. Initial conditions are inherited from the previous convective/flooding events, setting the brine to the underlying seawater composition ($Si(OH)_4 = 51$ µmol l^{-1} and $\delta^{30}Si = 1.8$ ‰ in Fripiat et al. 2007). We assume no external $Si(OH)_4$ supply between two consecutive convective/flooding events. While this is a very good approximation of reality in the interior of the ice and in its surface layer, as outlined in the previous section, there will be some exchange of brine with the underlying ocean close to the ice–ocean interface. This exchange is, however, limited, since otherwise measured $Si(OH)_4$ in the bottom community should be very similar to that of the underlying seawater. In the following, the effect of an additional input of silicic acid will be discussed for the bottom community. Si isotopes are consumed during biogenic silica production (P) with a fractionation factor of −1.2 ‰, and remineralized by biogenic silica dissolution (D) with a fractionation factor of −0.55 ‰ (De La Rocha et al. 2000, 2011; Varela et al. 2004; Cardinal et al. 2005; Reynolds et al. 2006; Beucher et al. 2008; Demarest et al. 2009; Cavagna et al. 2011; Fripiat et al. 2011). The mass and isotopic balance is given by:

$$dDSi/dt = -P + D \quad (3)$$

$$dbSiO_2/dt = P - D \quad (4)$$

$$\frac{dD^{30}Si}{dt} = -P \times \frac{D^{30}Si}{DSi} \times \left(1 + \frac{^{30}\varepsilon_P}{1000}\right) + D \times \frac{b^{30}SiO_2}{bSiO_2} \times \left(1 + \frac{^{30}\varepsilon_D}{1000}\right) \quad (5)$$

$$\frac{db^{30}SiO_2}{dt} = P \times \frac{D^{30}Si}{DSi} \times \left(1 + \frac{^{30}\varepsilon_P}{1000}\right) - D \times \frac{b^{30}SiO_2}{bSiO_2} \times \left(1 + \frac{^{30}\varepsilon_D}{1000}\right) \quad (6)$$

where DSi = silicic acid, $bSiO_2$ = biogenic silica, $^{30}\varepsilon_P$ = fractionation factor of $bSiO_2$ production, and $^{30}\varepsilon_D$ = fractionation factor of $bSiO_2$ dissolution. ^{30}Si concentrations are estimated from Eq. (1) and by using the approximation that the concentration of the most abundant Si isotopes (^{28}Si) is equal to Si concentration. For such level of silicic acid consumption, the errors associated with such approximation are negligible, i.e. lower than 0.01 ‰ (e.g. Fry 2006). The model is run for N time steps of length dt, producing at each time step an amount of $\int P/N\ (= P)$ and dissolving $\int D/N\ (= D)$, where $\int P$ and $\int D$ are the integrated $bSiO_2$ production and dissolution, respectively. We solve model differential equations for varying $bSiO_2$ production and dissolution rates, aiming to find the best agreement between the model {DSi (m), $\delta^{30}Si_{bSiO2}$ (m)} and the observations {DSi (i), $\delta^{30}Si_{bSiO2}$(i)}. To measure this agreement, we use the minimum cost function, searching for the lowest standardized residual (SR; Elskens et al. 2007; Fig. 3d):

$$SR = \frac{(DSi(i) - DSi(m))^2}{(\sigma_{DSi})^2} + \frac{(\delta^{30}Si_{bSiO2}(i) - \delta^{30}Si_{bSiO2}(m))^2}{(\sigma_{\delta 30Si})^2} \quad (7)$$

Here, $\sigma_{DSi} = 3$ µmol l^{-1} and $\sigma_{\delta 30Si} = 0.1$ ‰ express the total standard deviation of DSi and $\delta^{30}Si$, respectively. Standardized residuals allow us to overcome the problem of different scaling between two variables, in this case between the concentration and its isotopic composition. Standardized residuals for each combination of biogenic silica production and dissolution have been estimated (see Fig. 3d for the example of the bottom community). Satisfying solutions correspond to combinations of P and D that result in an SR lower than 1 (Fig. 3d). Results from all simulations with combinations of P and D that fulfill this criterion are presented in Fig. 3a–c. We find simulated $Si(OH)_4$ concentration and $\delta^{30}Si$ within the analytical error range of the observations (Fig. 3a, b). The sensitivity of the resulting $bSiO_2$ dissolution on the D:P ratio is shown in Fig. 3c.

In the bottom community (station IV), satisfying solutions are found with a D:P ratio varying between 0.4 and 0.8 and with the model best fit at 0.6 (cross in Fig. 3c). Overall, the D:P ratios were slightly larger in the two surface communities (not shown): between 0.7 and 0.8 (best fit = 0.8) for station V; between 0.5 and 0.9 (best fit = 0.7) for station III. This is sensible, given the easy access of seawater $Si(OH)_4$ to the bottom community. To test our assumption of a closed system for the bottom community, we ran the model by supplying 10 µmol l^{-1} of silicic acid ($\sim$20 % of initial $Si(OH)_4$ concentration). The resulting D:P ratio was slightly smaller (0.4) indicating that additional supply might lower the contribution of $bSiO_2$ dissolution to production there than we find based on our assumption of a closed system. Such D:P ratios are in the upper range of those encountered in the marine environments (from less than 0.1 to >0.5; Brzezinski et al. 2003), implying a sea ice Si-regenerated dynamic. Three processes can explain why sea ice appears to be a favorable environment for biogenic silica dissolution:

(1) Large accumulation of bacteria, including attached species, is commonly observed in sea ice (Thomas and Dieckmann 2002; Meiners et al. 2004). Hydrolyzing activity of bacteria removes the organic matrix from diatom frustules and exposes them to the ambient under-saturated brine environment (Bidle and Azam 1999).

(2) Frustules of dead diatoms remain enclosed in the tortuosity of the brine network, therefore increasing the residence time of biogenic silica in contact with the brine and hence its susceptibility to dissolution.

(3) As pointed out in (Thomas et al. 2010), shifts in pH to high values in highly productive sea ice assemblages (Gleitz et al. 1995; Delille et al. 2007) will significantly enhance the dissolution rate of frustules. However, such increase can be counterbalanced by low dissolution rates at low temperatures.

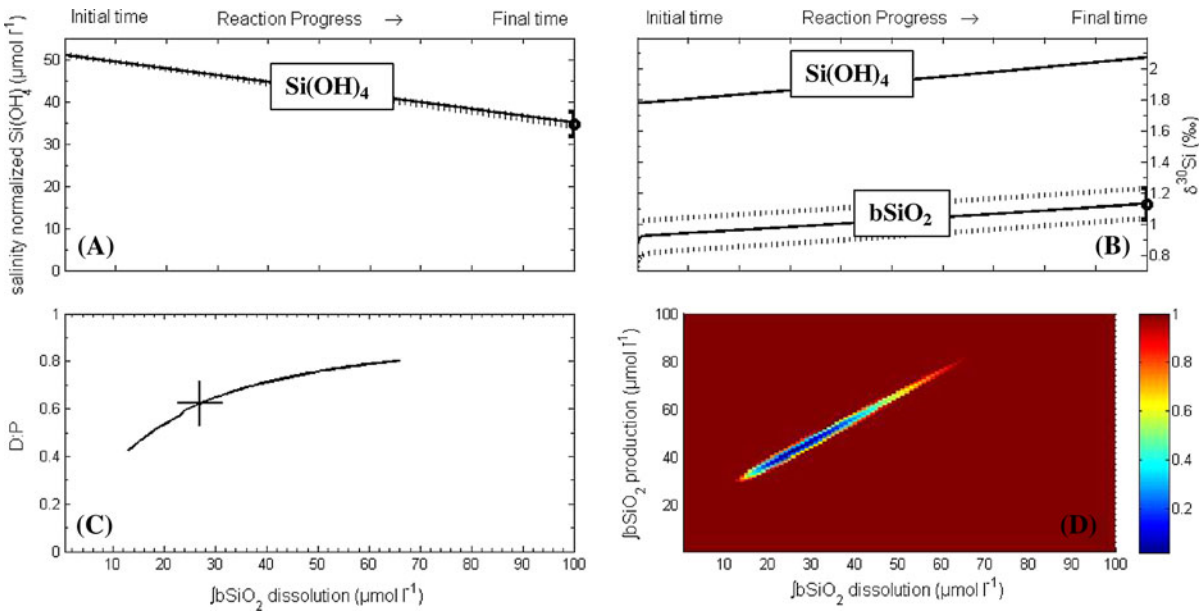

Fig. 3 Example of optimization for a bottom community in Antarctic pack ice (Fripiat et al. 2007). **a** Normalized silicic acid concentration for the model best fit (*full line*), the model envelope corresponding to the simulations with a standard residual lower than 1 (*dashed lines*), and the observations (*dot with error bars*). **b** δ^{30}Si for the model best fit (*full line*), the model envelope corresponding to the simulations with a standard residual lower than 1 (*dashed lines*), and the observations (*dot with error bars*). **c** D:P ratio corresponding to the simulation with a standard residual lower than 1 (*full line*) and for the model best fit (=lowest standard residual; *cross*). **d** Standard residuals (*color bar*) for each pair of integrated $bSiO_2$ production and dissolution. (Color figure online)

We acknowledge that such optimization is dependent on the values chosen for the fractionation factors. To test the sensitivity of our estimates, we ran the model with three different values for the fractionation factor associated with biogenic silica production (−0.9, −1.2, and −1.5 ‰), in agreement with field-based variability (−1.2 ± 0.3 ‰; De La Rocha et al. 2000, 2011; Varela et al. 2004; Cardinal et al. 2005; Reynolds et al. 2006; Beucher et al. 2008; Cavagna et al. 2011; Fripiat et al. 2011). We find significant sensitivity of the best estimates of D:P ratios in our simulations to the specific choice of the fractionation factor (Table 1), especially for the bottom community (Station IV). We cannot rule out that sea ice diatom assemblages fractionate Si-isotopes differently. Further studies have to increase the constraints on the mass and isotopic balances: e.g. to assess both δ^{30}Si of silicic acid and biogenic silica evolution. However, in this pilot study, biogenic silica dissolution was important in every scenario (D:P ratios > 0.4), except for the bottom community where relatively low D:P ratio (=0.2) are found for $^{30}\varepsilon_p = -0.9$ ‰ (Table 1).

Table 1 Sensitivity of the D:P ratio (best fit) to the fractionation factor for biogenic silica production ($^{30}\varepsilon_p$), from field-based variability (−1.2 ± 0.3 ‰)

$^{30}\varepsilon_p$ (‰)	D:P ratios per station		
	III	IV	V
−0.9	0.4	0.2	0.5
−1.2	0.7	0.6	0.8
−1.5	0.8	0.9	0.8

Conclusions

In order to use the natural silicon isotopic composition as a new tool to investigate sea ice biogeochemical dynamic, we need first to develop a mechanistic understanding of the processes driving its distribution. Winter sampling of newly formed Arctic landfast first-year sea ice allowed us to assess the initial setting of sea ice δ^{30}Si, before the building of biomass and associated biogenic silica production and dissolution processes. We have shown that abiotic physico-chemical processes,

associated with the building of sea ice, do not fractionate silicon isotope. Hence, initial δ^{30}Si depends only on the relative contribution of silicic acid sources (e.g. seawater and rivers for Arctic coastal environments). By knowing initial silicic acid δ^{30}Si, mass and isotopic balance can be solved to estimate biogenic silica production and dissolution, both with their specific fractionation factor. A first attempt on a previously published dataset in productive Antarctic pack ice from the Australian Southern Ocean sector points out a significant contribution of biogenic silica dissolution (D) to production (P), i.e. a D:P ratio between 0.4 and 0.9. Sea ice silicon biogeochemical dynamic implies therefore a significant regeneration of silicon within the brine network, fueling regenerated biogenic silica production. To our best knowledge no such informations exist today for sea ice. This is due to the fact that this environment is poorly suited for estimating rates based on manipulative techniques such as tracer incubations. The findings presented in this study bare significant implications for our understanding and parameterization of sea ice Si-cycling. In particular, we hope that based on our findings, the lack of a parameterization of silica dissolution in current sea-ice biogeochemical models (Vancoppenolle et al. 2010) will be overcome.

Acknowledgments Our warm thanks to the owner of the sailing vessel 'SS Dagmar Aaen', Arved Fuchs, and to Rémy Tokouda and Kai Maibaum for their support in the field. We are also grateful to Ivan Petrov and Nadine Mattielli for the management of the MC-ICP-MS laboratory at ULB; to L. Monin, N. Dahkani, J. Navez (RMCA) and S. El Amri (ULB) for their help in sample processing. This work was conducted within BELCANTO III-BIGSOUTH networks (contracts SD/CA/03A and SD/CA/05A of SPSDIII, Support Plan for Sustainable Development) funded by BELSPO, The Belgian Science Policy. François Fripiat thanks the COST Action ES0801 for the funding of a Short Term Scientific Mission. Luc André thanks the "Fonds National de la Recherche Scientifique" (FNRS, Belgium) for its financial support (FRFC project 2.4512.00). Bruno Delille is a research associated with the F.R.S.-FNRS. François Fripiat was and is a postdoctoral fellows with the F.R.S.-FNRS and Fonds Wetenschappelijk Onderzoek (FWO, Belgium), respectively. We are very grateful to all three reviewers for their insightful comments which helped us to significantly improve the manuscript.

References

Abraham K, Opfergelt S, Fripiat F, Cavagna A-J, de Jong JTM, Foley SF, André L, Cardinal D (2008) δ^{30}Si and δ^{29}Si determinations on USGS BHVO-1 and BHVO-2 reference materials with a new configuration on a Nu Plasma Multi-Collector ICP-MS. Geostand Geoanal Res 32(2):193–202

Arar EJ, Collins GB (1997) Method 445.0: in vitro determination of chlorophyll a and pheophytin a in marine and freshwater phytoplankton by fluorescence, National Exposure Research Laboratory, Office of Research and Development, U.S. Environmental Protection Agency

Arrigo KR, Thomas DN (2004) Large scale importance of sea ice biology in the Southern Ocean. Antarctic Sci 16(4): 471–486

Arrigo KR, Lizotte MP, Mock T (2010) Sea ice algae. In: Thomas DN, Dieckmann GS (eds) Sea ice. Blackwell Science Ltd., Oxford

Beucher CP, Brzezinski MA, Jones JL (2008) Source and biological fractionation of silicon isotopes in the Eastern Equatorial Pacific. Geochim Cosmochim Acta 72: 3063–3073

Bidle KD, Azam F (1999) Accelerated dissolution of diatom silica by marine bacterial assemblages. Nature 397: 508–512

Brzezinski MA, Jones JL, Bidle KD, Azam F (2003) The balance between silica production and silica dissolution in the sea: insights from Monterey Bay, California, applied to the global data set. Limnol Oceanogr 48(5):1846–1854

Cardinal D, Alleman LY, de Jong J, Ziegler K, André L (2003) Isotopic composition of silicon measured by multicollector plasma source mass spectrometry in dry plasma mode. J Anal At Spectrom 18:213–218

Cardinal D, Alleman LY, Dehairs F, Savoye N, Trull TW, André L (2005) Relevance of silicon isotopes to Si-nutrient utilization and Si-source assessment in Antarctic waters. Global Biogeochem Cycles 19:GB2007. doi:10.1029/2004GB002364

Cavagna A-J, Fripiat F, Dehairs F, Wolf-Gladrow D, Cisewski B, Savoye N, André L, Cardinal D (2011) Silicon uptake and supply during a Southern Ocean iron fertilization experiment (EIFEX) tracked by Si isotopes. Limnol Oceanogr 56(1):147–160

Cox GFN, Weeks WF (1983) Equations for determining the gas and brine volumes in sea-ice samples. J Glaciol 29(102): 306–316

de Brauwere A, Fripiat F, Cardinal D, Cavagna A-J, De Ridder F, André L, Elskens M (2012) Isotopic model of oceanic silicon cycling: the Kerguelen Plateau case study. Deep-Sea Res I 70:42–59

De La Rocha CL, Brzezinski MA, DeNiro MJ (1996) Purification recovery and laser-driven fluorination of silicon from dissolved and particulate silica for the measurement of natural stable isotope abundances. Anal Chem 68: 3746–3750

De La Rocha CL, Brzezinski MA, DeNiro MJ (1997) Fractionation of silicon isotopes by marine diatoms during biogenic silica formation. Geochim Cosmochim Acta 61(23):5051–5056

De La Rocha CL, Brzezinski MA, DeNiro MJ (2000) A first look at the distribution of the stable isotopes of silicon in natural waters. Geochim Cosmochim Acta 64(14):2467–2477

De La Rocha CL, Bescont P, Croguennoc A, Ponzevera E (2011) The silicon isotopic composition of surface waters in the Atlantic and Indian sectors of the Southern Ocean. Geochim Cosmochim Acta 75:5283–5295

Delille B, Jourdain B, Borges AV, Tison J-L, Delille D (2007) Biogas (CO_2, O_2, dimethylsulfide) dynamics in Spring

Antarctic fast ice. 52(4):1367–1379. Limnol Oceanogr 52(4):1367–1369

Demarest MS, Brzezinski MA, Beucher CP (2009) Fractionation of silicon isotopes during biogenic silica dissolution. Geochim Cosmochim Acta 73:5572–5583

Ehlert I (2012) On the evolution of first-year sea ice, Ph.D. Thesis. In: Max-Planck Institute for Meteorology, Hamburg, Germany. Available at http://www.mpimet.mpg.de/fileadmin/publikationen/Reports/WEB_BzE_122.pdf Accessed 26 Feb 2013

Elskens M, de Brauwere A, Beucher C, Corvaisier R, Savoye N, Tréguer P, Baeyens W (2007) Statistical process control in assessing production and dissolution rates of biogenic silica in marine environments. Mar Chem 106:272–286

Fripiat F, Cardinal D, Tison J-L, Worby A, André L (2007) Diatoms-induced Si-isotopic fractionation in Antarctic sea-ice. J Geophys Res 112:G02001. doi:10.1029/2006JC000244

Fripiat F, Cavagna A-J, Savoye N, Dehairs F, André L, Cardinal D (2011) Isotopic constraints on the Si-biogeochemical cycle of the Antarctic zone. Mar Chem 123:11–22

Fry B (2006) Stable isotope ecology. Springer, New York

Gleitz M, van der Loeff MR, Thomas DN, Dieckmann GS, Millero FJ (1995) Comparison of summer and winter inorganic carbon, oxygen and nutrient concentrations in Antarctic sea ice brine. Mar Chem 51:81–91

Gosselin M, Levasseur M, Wheeler PA, Horner RA, Booth BC (1997) New measurements of phytoplankton and ice algal production in the Arctic Ocean. Deep-Sea Res II 41(8):1623–1644

Griewank PJ, Notz D (2013) Insights into brine dynamics and sea ice desalination from a 1-D model study of gravity drainage. J Geophys Res Oceans 118(7):3370–3386. doi:10.1002/jgrc.20247

Horner R, Schrader GC (1982) Relative contributions of ice algae, phytoplankton, and benthic microalgae to primary production in nearshore regions of the Beaufort Sea. Arctic 36(4):485–503

Jardon FP, Vivier F, Vancoppenolle M, Lourenco A, Bouruet-Aubertot P, Cuypers Y (2013) Full-depth desalination of warm sea ice. J Geophys Res Oceans 118:435–447. doi:10.1029/2012JC007962

Lee SH, Whitledge TE, Kang S-H (2008) Spring time production of bottom ice algae in the landfast sea ice zone at Barrow. Alaska J Exp Mar Biol Ecol 367:204–212

Legendre L, Ackley SF, Dieckmann GS, Gulliksen B, Horner R, Hoshiai T, Melnikov IA, Reeburgh WS, Spindler M, Sullivan CW (1992) Ecology of sea ice biota 2. Global significance. Polar Biol 12:429–444

Meiners K, Brinkmeyer R, Granskog MA, Lindfors A (2004) Abundance, size distribution and bacterial colonization of exopolymer particles in Antarctic sea ice (Bellingshausen Sea). Aquat Microb Ecol 35:283–296

Notz D, Worster MG (2009) Desalination processes of sea ice revisited. J Geophys Res 114:C05006. doi:10.1029/2008JC004885

Petrich C, Langhorne PJ, Sun ZF (2006) Modelling the interrelationships between permeability, effective porosity and total porosity in sea ice. Cold Reg Sci Tech 44:131–144. doi:10.1016/j.coldregions.2005.10.001

Reynolds BC, Frank M, Halliday AN (2006) Silicon isotope fractionation during nutrient utilization in the North Pacific. Earth Planet Sci Lett 244:431–443

Reynolds BC, Aggarwal J, André L, Baxter D, Beucher C, Brzezinski MA, Engström E, Georg BR, Land M, Leng MJ, Opfergelt S, Rodushkin I, Sloane HJ, van den Boorn HJM, Vroon PZ, Cardinal D (2007) An inter-laboratory comparison of Si isotope reference materials. J Anal At Spectrom 22:561–568

Riedel A, Michel C, Gosselin M, Leblanc B (2008) Winter–spring dynamics in sea-ice carbon cycling in the coastal Arctic Ocean. J Mar Syst 74:918–932

Sigman DM, Karsh KL, Casciotti KL (2009) Nitrogen isotopes in the ocean. In: Steele JH, Turekian KK, Thorpe SA (eds) Encyclopedia of ocean sciences (update from 2001). Academic Press, London, pp 4138–4153

Sutton JN, Varela DE, Brzezinski MA, Beucher CP (2013) Species-dependent silicon isotope fractionation by marine diatoms. Geochim Cosmochim Acta 104:300–309

Thomas DN, Dieckmann GS (2002) Antarctic sea ice—a habitat for extremophiles. Science 295:641–645

Thomas DN, Papadimitriou S, Michel C (2010) Biogeochemistry of sea ice. In: Thomas DN, Dieckmann GS (eds) Sea ice. Blackwell Science Ltd., Oxford

Vancoppenolle M, Goosse H, de Montety A, Fichefet T, Tremblay B, Tison J-L (2010) Modeling brine and nutrient dynamics in Antarctic sea ice: the case of dissolved silica. J Geophys Res 115:C02005. doi:10.1029/2009JC005369

Varela DA, Pride CJ, Brzezinski MA (2004) Biological fractionation of silicon isotopes in Southern Ocean surface waters. Global Biogeochem Cycles 18:GB1047. doi:10.1029/2003GB002140

Worster MG, Wettlaufer JS (1997) Natural convection, solute trapping, and channel formation during solidification of saltwater. J Phys Chem B 101:6132–6136